



## Silver infiltrated $\text{La}_{0.6}\text{Sr}_{0.4}\text{Co}_{0.2}\text{Fe}_{0.8}\text{O}_3$ cathodes for intermediate temperature solid oxide fuel cells

Y. Sakito<sup>a</sup>, A. Hirano<sup>a</sup>, N. Imanishi<sup>a</sup>, Y. Takeda<sup>a,\*</sup>, O. Yamamoto<sup>a</sup>, Y. Liu<sup>b</sup>

<sup>a</sup> Department of Chemistry for Materials, Graduate School of Engineering, Mie University, 1577 Kurima-machia-cho, Tsu, Mie 514-8507, Japan

<sup>b</sup> Shanghai Institute of Ceramics, Chinese Academy of Science, 1295 Ding Xi Road, Shanghai 200050, China

### ARTICLE INFO

#### Article history:

Accepted 21 April 2008

Available online 30 April 2008

#### Keywords:

SOFC

LSCF

GDC composite electrode

Ag-electrode

Infiltration method

### ABSTRACT

Porous  $\text{La}_{0.6}\text{Sr}_{0.4}\text{Co}_{0.2}\text{Fe}_{0.8}\text{O}_3$  (LSCF) electrodes on anode support cells were infiltrated with  $\text{AgNO}_3$  solutions in citric acid and ethylene glycol. Two types of solid oxide fuel cells with the LSCF–Ag cathode, Ni–YSZ/YSZ/LSCF–Ag and Ni– $\text{Ce}_{0.9}\text{Gd}_{0.1}\text{O}_{1.95}$ (GDC)/GDC/LSCF–Ag, were examined in a temperature range 530–730 °C under air oxidant and moist hydrogen fuel. The infiltration of about 18 wt.% Ag fine particles into LSCF resulted in the enhancement of the power density of about 50%. The maximum power density of Ni–YSZ/YSZ/LSCF was enhanced from 0.16  $\text{W cm}^{-2}$  to 0.25  $\text{W cm}^{-2}$  at 630 °C by infiltration of  $\text{AgNO}_3$ . No significant degradation of out-put power was observed for 150 h at 0.7 V and 700 °C. The Ni–GDC/GDC/LSCF–Ag cell showed the maximum power density of 0.415  $\text{W cm}^{-2}$  at 530 °C.

© 2008 Elsevier B.V. All rights reserved.

### 1. Introduction

Solid oxide fuel cells (SOFCs) are attractive electric power generation system with high-energy conversion efficiency as high as 60% for electricity and 80% for electricity and thermal energy. In addition, SOFCs have many advantages such as multi-fuel capability and simplicity of system design [1,2]. The high efficiency will contribute to reduce  $\text{CO}_2$  emission. SOFCs have been extensively developed for more than 40 years and the practical SOFC systems with a high performance have demonstrated already. The cost performance, however, has not been acceptable for the commercial applications. At moment, the most successful SOFCs have been operated at 1000 °C. To reduce the costs, lowering of the SOFC operation temperatures has been widely pursued to extend the materials selection to suppress the degradation of SOFC components and consequently to extend the cell lifetime [3]. Inexpensive metallic materials may be used for interconnect and manifold components at an operating temperature lower than 800 °C [4]. However, the SOFC performance decreases with decreasing the operation temperature, because of increasing the electrode polarization and the electrolyte resistance. The electrolyte resistance contribution can be reduced significantly by using a thin film electrolyte on an anode support structure [5] and high conductivity oxide ion conductors

such as the doped  $\text{LaGaO}_3$  [6] and scandia doped zirconia [7]. While improvements in electrolyte for low temperature SOFCs have been achieved, their performance is still typically limited by cathode polarization. Thus, there is interest in identifying improved cathodes for low-to-medium temperature SOFCs.

$\text{La}_{0.6}\text{Sr}_{0.4}\text{Co}_{0.2}\text{Fe}_{0.8}\text{O}_3$  (LSCF) is a promising cathode material in SOFCs operating intermediate temperature (550–750 °C) [8]. Sahibzada et al. reported the cell performance of the Ni– $\text{Ce}_{0.9}\text{Gd}_{0.1}\text{O}_{1.95}$ (GDC)/GDC/LSCF cell in a temperature range 650–550 °C [9]. The maximum out-put power of 140  $\text{mW cm}^{-2}$  and 80  $\text{mW cm}^{-2}$  was observed at 650 °C and 600 °C, respectively. The addition of noble metals to porous SOFC electrodes is known to improve the electrocatalytic activity. Generally these noble metals were introduced by wet infiltration method [9–11]. Sahibzada et al. [9] investigated the effect of the addition of Pd to the LSCF cathode and found to decrease the over all cell resistance by 15.5% at 650 °C and 40% at 550 °C. However, the performance of the cell with Pd addition deteriorated very first [12]. Silver metal is an excellent candidate for the cathode in SOFCs with operating at less than 800 °C, because of its good catalytic activity, high electrical conductivity and its relatively low cost. Wang et al. reported the oxygen reduction catalytic activity of the LSCF–CGO–Ag composite electrode [13]. The addition of  $\text{AgNO}_3$  solution into the LSCF–CGO composite electrode improved the catalytic activity for oxygen reduction; Liu et al. [14] reported the effect of the Ag addition into LSCF–GDC. The power density of

\* Corresponding author. Tel.: +81 59 231 9419; fax: +81 59 231 9478.  
E-mail address: [takeda@chem.mie-u.ac.jp](mailto:takeda@chem.mie-u.ac.jp) (Y. Takeda).

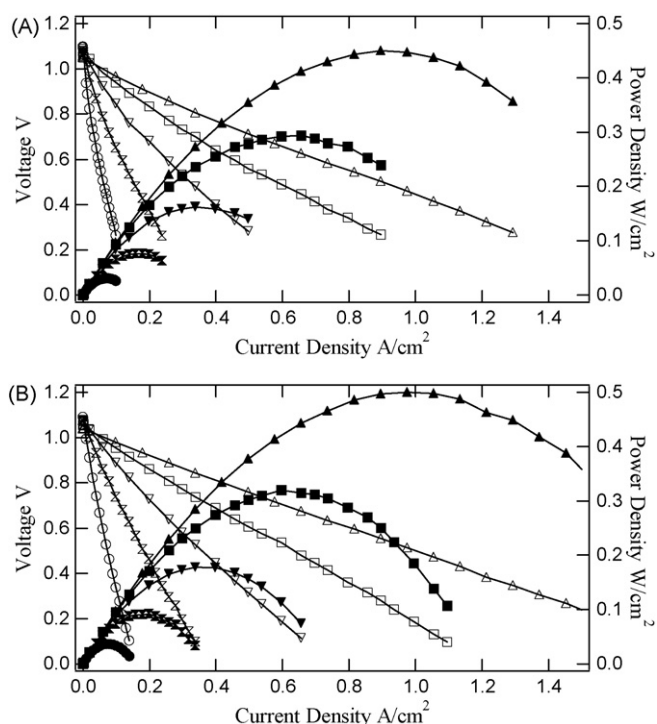


**Fig. 1.** Current–voltage curves of Ni–YSZ/YSZ/GDC/LSCF (A) and Ni–YSZ/YSZ/GDC/Ag infiltrated LSCF by a  $\text{AgNO}_3$  aqueous solution (B) under moist  $\text{H}_2$  fuel and air at various temperatures. ( $\Delta$ ,  $\blacktriangle$ ) 730 °C; ( $\square$ ,  $\blacksquare$ ) 680 °C; ( $\nabla$ ,  $\blacktriangledown$ ) 630 °C; ( $\otimes$ ,  $\otimes$ ) 580 °C; ( $\circ$ ,  $\bullet$ ) 530 °C.

the Ni– $(\text{ZrO}_2)_{0.89}(\text{Sc}_2\text{O}_3)_{0.1}(\text{CeO}_2)_{0.01}(\text{ScSZ})/\text{ScSZ}/\text{GDC}/\text{LSCF}$  cell at 0.7 V and 550 °C was enhanced  $60 \text{ mW cm}^{-2}$  to  $300 \text{ mW cm}^{-2}$  by Ag impregnation. In this study, the various types of the solution containing Ag was infiltrated into the LSCF cathode and the SOFC performance of the anode supported cell with the cathode was examined in a temperature range 730–530 °C.

## 2. Experimental

The LSCF and GDC powders were purchased from Semi Chemical, Japan. The two type anode support half cells, Ni–YSZ/YSZ (21 mm in diameter, 500  $\mu\text{m}$  in total thickness, and  $\sim 15 \mu\text{m}$  in electrolyte thickness) and Ni–GDC/GDC (21 mm in diameter, 500  $\mu\text{m}$  in total thickness, and  $\sim 15 \mu\text{m}$  in electrolyte thickness) were supplied from Hosokawa Micron Co., Japan. To protect the reaction of YSZ and LSCF, a GDC film was screen-printed on the YSZ electrolyte and then sintered at 1200 °C for 4 h. The thickness of the GDC layer was about 7  $\mu\text{m}$ . The LSCF and polyethylene glycol (molecular weight: 190–210) mixture (70:30 weight ratio) was screen-printed on the GDC surfaces of the Ni–YSZ/YSZ/GDC and Ni–GDC/GDC cells and sintered at 1100 °C for 4 h. The thickness of the LSCF layer was about 15  $\mu\text{m}$ . The active area of the cathode was 0.5  $\text{cm}^2$ . The power density of the cells was calculated from based on the cathode active area.

The polymerized complex method is an effective technique to obtain a homogenous fine particle [15]. This method is based on the Pechini's process consisting in formation of complex of the respective metals with hydroxypolycarboxylic acid in ethylene glycol (EG) medium. Citric acid and glycine were used as the hydroxypolycarboxylic acid. A weighted amount of citric acid or glycine was dissolved in a measured volume of ethylene glycol under stirring and heating at 40 °C, and then silver nitrate was added to the obtained solution. The solution with silver

nitrate was infiltrated into the porous LSCF electrode and heated at 200 °C for 2 h. To obtain  $\text{Ag}_{0.8}\text{Pd}_{0.2}$  alloy, the mixed solution of  $\text{Pd}(\text{NO}_3)_2$  and  $\text{AgNO}_3$  (2:8 mol ratio) in citric acid and EG were used.

The anode support cell was set upped in a ProbeState™ (Norwegian Electro Ceramics AS, Norway). A silver ring was used as the gas sealing at the anode. Fuel cell tests were carried out in a temperature range 530–730 °C using a wet  $\text{H}_2$  fuel (bubbled in water at 25 °C) in excess on the anode side and air in excess on the cathode side. The open-circuit voltages of the test cells were much closed with the calculated values. That is, the gas sealing was well. The cell voltages were measured under a constant current drain. The cell impedance was measured using a Solartron 1260 analyzer and Solartron 1287 electrochemical interface in the frequency range  $10^6$  to 0.05 Hz with amplitude of 10 mV.

XRD patterns were collected with a Rotaflex RU 200B with  $\text{Cu K}\alpha$  radiation. The cathode morphologies were characterized with a Hitachi S4000 scanning electron microscope (SEM) and the distributions of elements in the cathode with a JEOL JXA8900R electron probe microanalysis (EPMA).

## 3. Results and discussion

The aqueous solution of  $\text{AgNO}_3$  ( $0.5 \text{ mol l}^{-1}$ ) was infiltrated into the porous LSCF cathode. The amount of silver in LSCF was about 18 wt.% to LSCF. Fig. 1 shows the current–voltage curves of the anode support Ni–YSZ/YSZ/GDC/LSCF cells with the Ag infiltrated LSCF cathode and the Ag free LSCF cathode in the temperature range 530–730 °C. The improvement of the power density by the Ag infiltration is remarkable at lower temperatures. The enhancements of maximum power density by infiltration of Ag are 20% at 530 °C, but only 10% at 730 °C. The SEM image and the element distribution map images of the close section of the Ag infiltrated LSCF cathode are shown in Fig. 2, where the samples were heated at 700 °C for 2 h. The distribution of Ag is not homogenous and the large amount of Ag is penetrated into the GDC layer.

To obtain a homogenous distribution of Ag over the LSCF matrix, the polymerized complex method was effective [14]. A solution of  $\text{AgNO}_3$  in citric acid and EG (2.26:1 weight ratio) was infiltrated into the LSCF matrix and heated at 700 °C for 2 h. As shown in Fig. 3, the polymerized complex method gives homogeneously distributed fine silver particles over the LSCF matrix. The particle size of Ag is less than 2  $\mu\text{m}$ . As expected, the fuel cell performances of the cell with this cathode are improved by fine silver particle distribution over the porous LSCF matrix as shown in Fig. 4. The maximum power densities are recorded as  $0.74 \text{ W cm}^{-2}$  at 730 °C and  $0.05 \text{ W cm}^{-2}$  at 530 °C, these values of which are more than 1.5 times compared to that of the LSCF cathode without Ag. The effect of the fine silver particle for the oxygen reduction was also reported previously. Wang and Barnett [16] found that the interfacial resistance of  $\text{La}_{0.7}\text{Co}_{0.3}\text{O}_3(\text{LSC})/(\text{Y}_2\text{O}_3)_{0.25}(\text{Bi}_2\text{O}_3)_{0.75}$  at 750 °C decrease from 0.7  $\Omega \text{ cm}^2$  to 0.5  $\Omega \text{ cm}^2$  by addition of 30% volume fraction Ag, where Ag was co-sputtered with LSC.

The power density of  $0.55 \text{ W cm}^{-2}$  at 0.7 V and 730 °C is attractive for the cathode in intermediate temperature fuel cells. This power density is compared to the results of by Murray et al. [17]. They claimed that the anode support Ni–YSZ/YSZ/LSCF–GDC cell showed good stability over entire 100 h test at 700 °C at 0.6 V and a power density of  $\sim 0.35 \text{ W cm}^{-2}$ . Sahibzada et al. [9] reported that performance enhancement was observed for Pd-impregnated LSCF cathode. However, the performance of the cell with Pd addition in the  $(\text{La}_{0.8}\text{Sr}_{0.2})_x\text{FeO}_3\text{–Ce}_{0.8}\text{Sm}_{0.2}\text{O}_{1.9}$  cathode deteriorated very fast; the power density measured at 0.7 V and 730 °C decreased from 0.61 to  $<0.4 \text{ W cm}^{-2}$  in less than 24 h [12]. In this study, long-

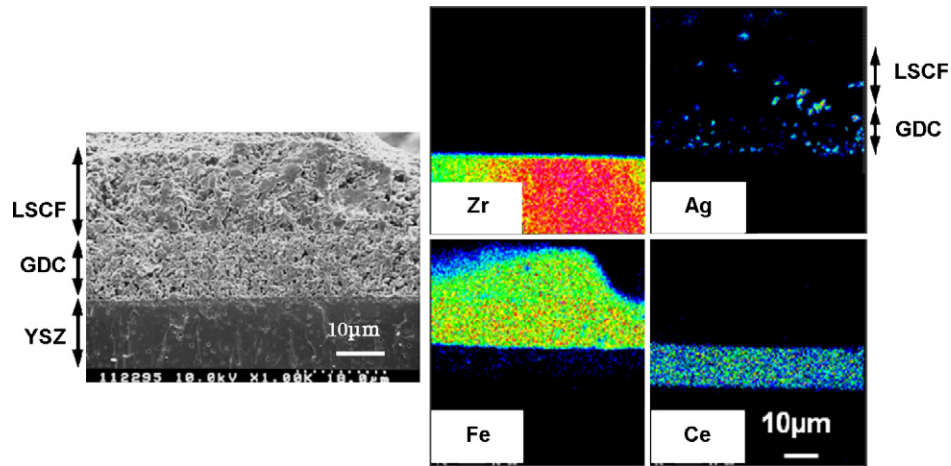


Fig. 2. SEM image and element distribution maps of the close section of the LSCF–GDC cathode Ag infiltrated from a  $\text{AgNO}_3$  aqueous solution (color online).

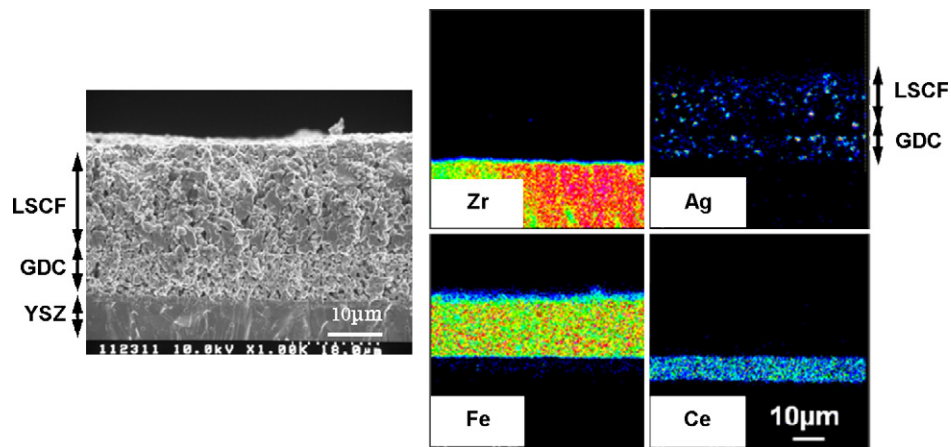


Fig. 3. SEM images and element distribution maps of the LSCF cathode Ag infiltrated from a  $\text{AgNO}_3$  solution in citric acid and EG (color online).

term cell performance tests have been carried out, and the changes of the power density with operation time are shown in Fig. 5. No significant power density change is observed within 150 h operation period. The impedance spectra of Ni–YSZ/YSZ/GDC/LSCF–Ag of the initial and after 150 h at  $730^\circ\text{C}$  are shown in Fig. 6. The ohmic resistance (intercept of the real axis at a high frequency) and the electrode polarization resistances are slightly decreased after operating for 150 h. The impedance plots show the two semicircles. The

low frequency semicircle was increased and the high frequency semicircle was not changed with decreasing the  $\text{H}_2$  concentration at the anode site. These results suggested that the low frequency semicircle and the high frequency semicircle are due to the contribution of the air electrode and of the fuel electrode, respectively, the LSCF–Ag electrode polarization resistance is rather decrease by operating for 150 h. That is, the LSCF cathode infiltrated Ag by the  $\text{AgNO}_3$  solution in citric acid and EG is stable at least for 150 h. The slightly decrease of the power density after 150 h operation

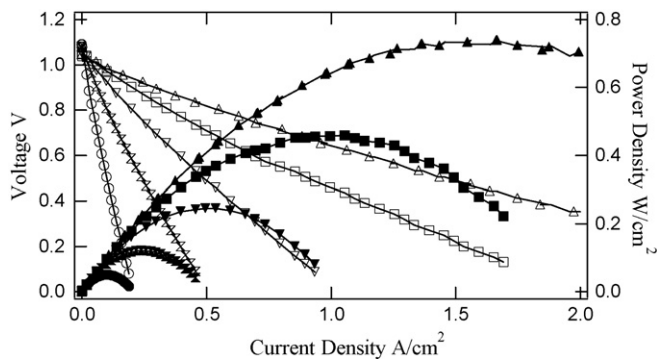


Fig. 4. Current–voltage curves of SOFC under moist  $\text{H}_2$  fuel with Ni–YSZ anode, YSZ electrolyte ( $15\ \mu\text{m}$ ), and Ag infiltrated LSCF cathode from a  $\text{AgNO}_3$  solution in citric acid and EG at various temperatures. ( $\Delta$ ,  $\blacktriangle$ )  $730^\circ\text{C}$ ; ( $\square$ ,  $\blacksquare$ )  $680^\circ\text{C}$ ; ( $\nabla$ ,  $\blacktriangledown$ )  $630^\circ\text{C}$ ; ( $\times$ ,  $\otimes$ )  $580^\circ\text{C}$ ; ( $\circ$ ,  $\bullet$ )  $530^\circ\text{C}$ .

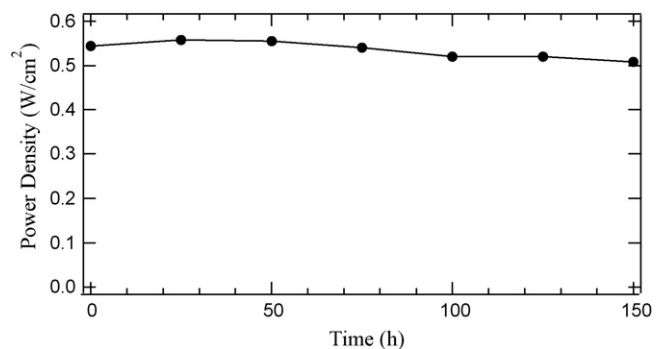


Fig. 5. Time dependence of the power density at  $700^\circ\text{C}$  and  $0.7\ \text{V}$  for a Ni–YSZ/YSZ/GDC/LSCF Ag infiltrated from a  $\text{AgNO}_3$  solution in citric acid and EG.

may be due to the crack in the thin film electrolyte, which was confirmed from the OCV decrease after 150 h operation. The OCV slightly decreased with operating time after 75 h. More long-term stability test is now in our research program.

Glycine is also used as the polymerized complex former with metal. The solution of  $\text{AgNO}_3$  in glycine and EG was infiltrated into the porous LSCF matrix and fired at  $700^\circ\text{C}$  for 2 h. The SEM image showed the smaller particle size of Ag than that from the citric acid solution, but Ag was distributed mainly on the GDC layer as shown in Fig. 7. The solubility of  $\text{AgNO}_3$  into the glycine and EG was not high and the solution of  $0.5 \text{ mol AgNO}_3 \text{ l}^{-1}$  was used. The total amount of Ag in LSCF was same as about 18 wt.% to LSCF. The  $\text{AgNO}_3$  solution may penetrate into the GDC layer.

The melting point of  $\text{Ag}_{0.8}\text{Pd}_{0.2}$  alloy ( $1100^\circ\text{C}$ ) is higher than that of Ag ( $960^\circ\text{C}$ ). So, we have tried to infiltrate  $\text{Ag}_{0.8}\text{Pd}_{0.2}$  into the LSCF matrix. The mixed solution of  $\text{AgNO}_3$  and  $\text{Pd}(\text{NO}_3)_2$  in citric acid and EG was infiltrated into the LSCF matrix and then was fired at  $700^\circ\text{C}$  for 1 h. The XRD patterns showed the formation of  $\text{Ag}_{0.8}\text{Pd}_{0.2}$ . The SEM image and elements distribution map image are shown in Fig. 8. The fine silver particles are distributed over the GDC buffer layer and the porous LSCF electrode. In Fig. 9, the SOFC performances of the cells with silver infiltrated from the various silver solutions were summarized at  $730^\circ\text{C}$ . The highest power density is observed in the cell with Ag infiltrated from the  $\text{AgNO}_3$  solution in citric acid and EG. The high performance could be explained by the homogenous distribution of the fine Ag particles over the LSCF matrix. The fine  $\text{Ag}_{0.8}\text{Pd}_{0.2}$  particles were homoge-

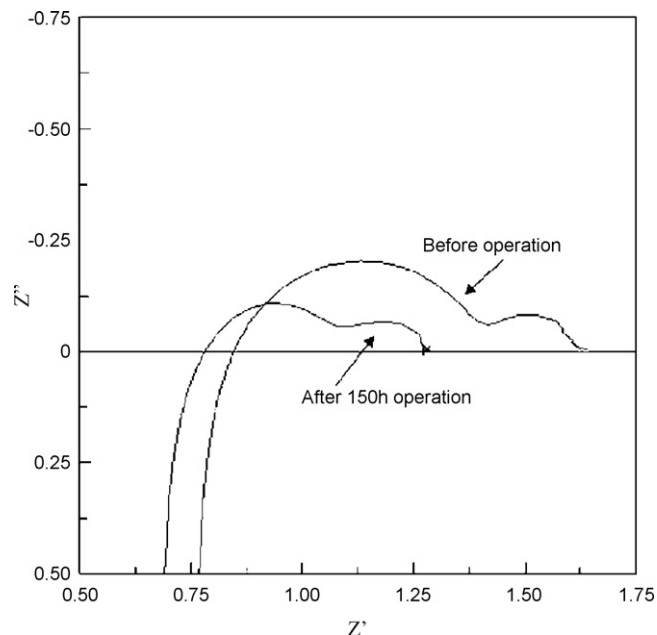


Fig. 6. Impedance spectra of Ni-YSZ/YSZ/GDC/LSCF-Ag before operation (A) and after 150 h operation (B) at  $730^\circ\text{C}$ .

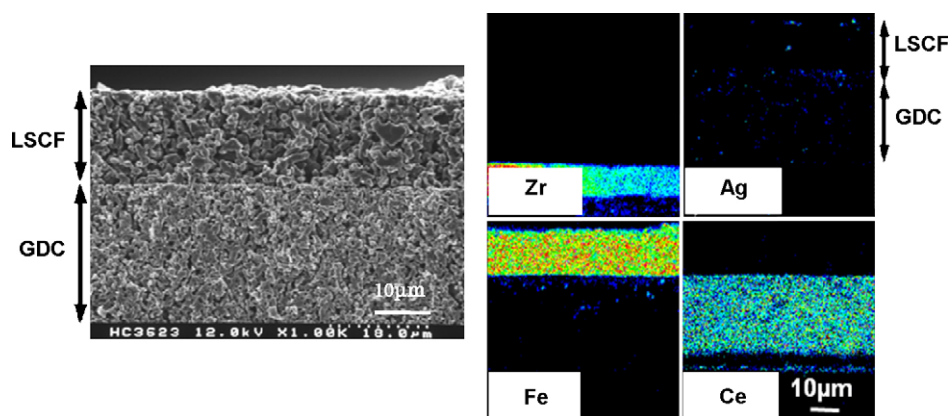


Fig. 7. SEM image and element distribution maps of LSCF Ag infiltrated from the  $\text{AgNO}_3$  solution in glycine and EG (color online).

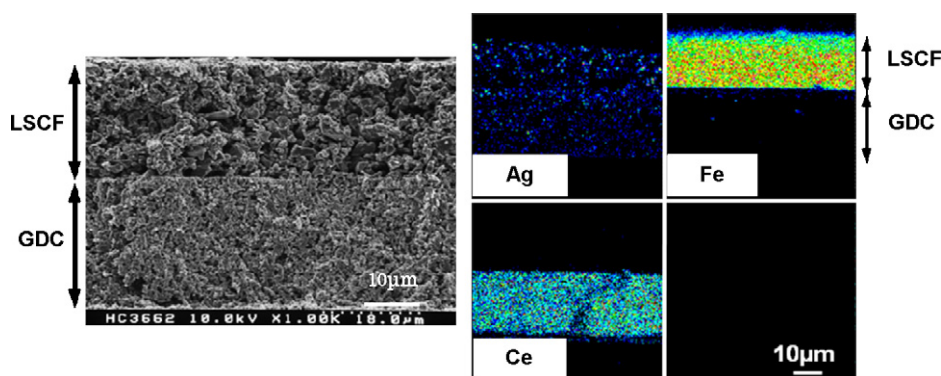
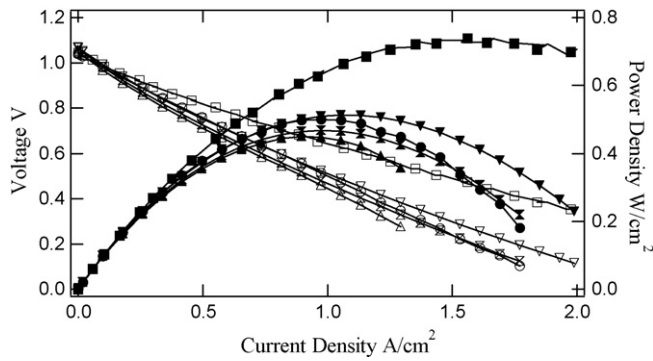


Fig. 8. SEM image and element distribution maps of the LSCF cathode Ag infiltrated from a  $\text{AgNO}_3\text{-Pd}(\text{NO}_3)_2$  solution in citric acid and EG (color online).





**Fig. 9.** Current–voltage curves of SOFC with the LSCF cathode Ag infiltrated from various Ag solutions at 680 °C. (□, ■) AgNO<sub>3</sub> in citric acid and EG; (▽, ▼) AgNO<sub>3</sub> + Pd(NO<sub>3</sub>)<sub>2</sub>; (○, ●) AgNO<sub>3</sub> in AgNO<sub>3</sub> in H<sub>2</sub>O; (△, ▲) LSCF without Ag; (⊠, ⊡) AgNO<sub>3</sub> in glycine and EG.

nously distributed over the LSCF matrix, but the cell performance with LSCF–Ag<sub>0.8</sub>Pd<sub>0.2</sub> was not improved as that with LSCF–Ag. The oxygen reduction catalytic activity of Ag<sub>0.8</sub>Pd<sub>0.2</sub> was not so high compared to Ag.

The doped ceria electrolytes have been used in low temperature SOFCs. The doped ceria, however, shows high electronic conductivity at higher temperature under reduces atmosphere [2]. At lower temperatures (<600 °C), loss of the energy conversation efficiency by the contribution of electronic conduction is reduced [18]. The high performance Ag infiltrated LSCF cathode was examined in SOFCs with the GDC electrolyte. The LSCF and EG mixture was screen-printed on the anode support GDC electrolyte (150 μm thick) and heated 1100 °C for 4 h, and then the AgNO<sub>3</sub> solution in citric acid and EG was infiltrated into the porous LSCF matrix. The SEM image and the element distribution map images are shown in Fig. 10, where the cathode was heated at 700 °C for 2 h. The Ag fine particles are distributed homogeneously over the porous LSCF matrix. In Fig. 11, the current–voltage curves at various temperatures for the Ni–GDC/GDC/LSCF cells with and without Ag fine particles in LSCF are shown. The maximum power densities of 0.32 W cm<sup>-2</sup> at 530 °C and 0.51 W cm<sup>-2</sup> at 580 °C are observed in the cell with the LSCF cathode. The OCVs at 530 °C and 630 °C were 0.98 V and 0.91 V, respectively, which are slightly lower than those calculated. The low OCV is due to the contribution of the electronic conduction in CGO. Doshi et al. [19] reported the similar results that the maximum power density of 0.14 W cm<sup>-2</sup> in the anode support cell with the LSCF cathode at 500 °C, where the GDC thickness was 30 μm. By Ag infiltration into the porous LSCF cathode, the SOFC performance was enhanced; the maximum power density at 530 °C is 0.42 W cm<sup>-2</sup> and that at 570 °C is 0.73 W cm<sup>-2</sup>. The power

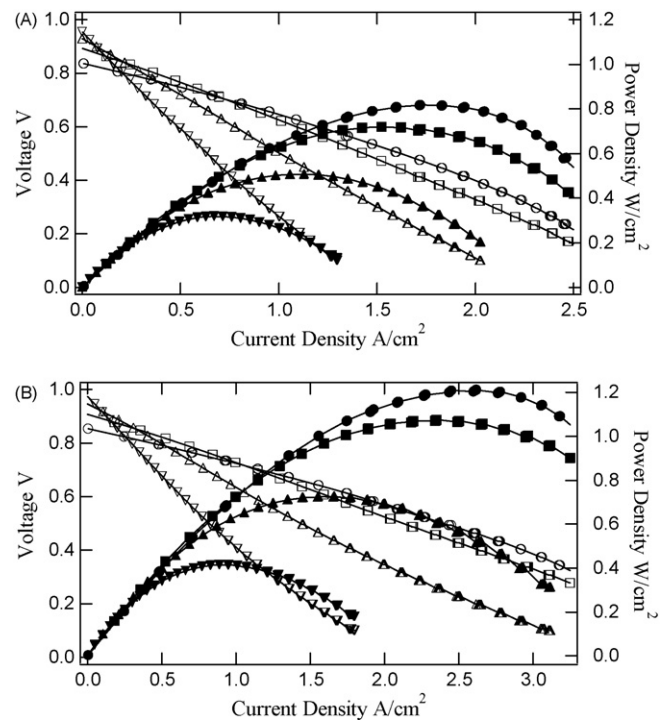


**Fig. 11.** Current–voltage curves of the Ni–GDC/GDC/LSCF without Ag (A) and with Ag (B) cells at various temperatures. (○, ●) 680 °C; (□, ■) 630 °C; (△, ▲) 580 °C; (▽, ▼) 530 °C.

density could be explained the low cathode polarization resistance of the LSCF–Ag cathode. The polarization resistance of the LSCF electrode at 530 °C was reduced from 0.63 Ω cm<sup>2</sup> to 0.46 Ω cm<sup>2</sup> by infiltration of AgNO<sub>3</sub>. The high performance cathode at lower temperatures is quite attractive for the intermediate temperature SOFC operating lower than 600 °C.

#### 4. Conclusions

The silver fine particles was distributed by the infiltration technique using the AgNO<sub>3</sub> solution in citric acid and EG. The anode support Ni–YSZ/YSZ/GDC/LSCF and Ni–GDC/GDC/LSCF cell performances were found to enhance by about 18% Ag infiltration into the porous LSCF cathode in a temperature range 530–730 °C. The long-term stability test showed no electrode performance degradation during 150 h operation. The high power density of 0.42 W cm<sup>-2</sup> at 530 °C in the Ni–GDC/GDC/LSCF–Ag cell is attractive for the intermediate temperature SOFC.

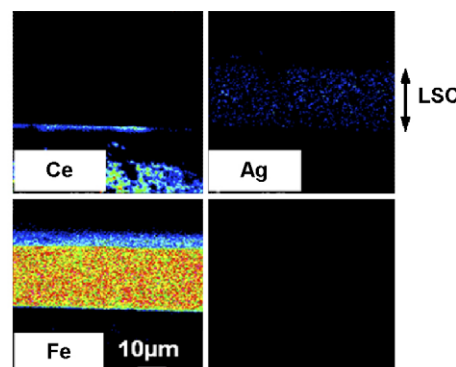
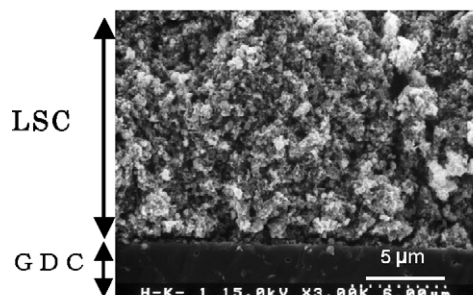


**Fig. 10.** SEM image and element distribution maps of the LSCF cathode Ag infiltrated from a AgNO<sub>3</sub> solution in citric acid and EG on Ni–GDC/GDC (color online).

## Acknowledgments

This work has been supported by NEDO, Japan as part of the Advanced Ceramic Reactor Project. The authors thank Drs. Fukui and Misono of Hosokawa Micron Co. for supplying the anode support cells and their valuable discussion.

## References

- [1] N.Q. Minh, T. Takahashi, *Science and Technology of Ceramic Fuel Cells*, Elsevier, Amsterdam, 1995.
- [2] O. Yamamoto, *Electrochem. Acta* 45 (2000) 2423.
- [3] C. Lu, T.Z. Sholkapper, C.P. Jacobson, S.J. Visco, J.C. De Jonghe, *J. Electrochem. Soc.* 153 (2006) A1115.
- [4] B.C.H. Steele, A. Heinzel, *Nature* 414 (2001) 345.
- [5] K. Kendall, N.Q. Minh, S.C. Singhal, in: S.C. Singhal, K. Kendal (Eds.), *High Temperature Solid Oxide Fuel Cells*, Elsevier, 2003 (Chapter 8).
- [6] T. Ishihara, H. Masuda, Y. Takita, *J. Am. Chem. Soc.* 116 (1994) 3801.
- [7] Y. Arachi, H. Sakai, O. Yamamoto, Y. Takeda, N. Imanishi, *Solid State Ionics* 121 (1999) 133.
- [8] L.W. Tai, M.M. Narsarallah, H.U. Anderson, D.M. Sparin, S.R. Sehlin, *Solid State Ionics* 76 (1995) 273.
- [9] M. Sahibzada, S.J. Benson, R.A. Rudkin, J.A. Kilner, *Solid State Ionics* 113/115 (1995) 285.
- [10] S.P. Jiang, *Mater. Sci. Eng. A* 418 (2006) 199.
- [11] H. Uchida, N. Mochizuki, M. Watanabe, *J. Electrochem. Soc.* 143 (1996) 1700.
- [12] S.P. Simmer, J.F. Bonnett, N.I. Candfield, K.D. Membradt, J.P. Shelton, V.L. Sprenkel, J.W. Stevenson, *J. Power Sources* 113 (2003) 1.
- [13] S. Wang, T. Kato, S. Nagata, T. Honda, T. Kaneko, N. Iwashita, M. Dokiya, *Solid State Ionics* 146 (2002) 203.
- [14] Y. Liu, M. Mori, Y. Funahashi, Y. Fujishiro, A. Hirano, *Electrochem. Commun.* 9 (2007) 1918.
- [15] M. Kakihana, *J. Sol-Gel Technol.* 6 (1996) 7.
- [16] L.S. Wang, S.A. Barnett, *Solid State Ionics* 76 (1995) 103.
- [17] E.P. Murray, M.J. Sever, S.A. Barnett, *Solid State Ionics* 148 (2002) 27.
- [18] M. Godlickemeier, L.J. Gauckler, *J. Electrochem. Soc.* 145 (1998) 414.
- [19] R. Doshi, V.L. Richard, J.D. Carter, X. Wang, M. Krumperut, *J. Electrochem. Soc.* 146 (1999) 1273.